G23A-0886

Compact Adaptable Mobile LiDAR System Deployment

Craig L. Glennie[1], Benjamin A. Brooks[2], Todd L. Ericksen[2], Darren Hauser[1], Kenneth W. Hudnut[3], James H. Foster[2], Jon Avery[2]

1. Department of Civil & Environmental Engineering, University of Houston, Houston, TX (clglennie@uh.edu)
2. School of Ocean & Earth Science & Technology, University of Hawaii, Honolulu, HI (bbrooks@hawaii.edu)
3. United States Geological Survey, Pasadena, CA (hudnut@usgs.gov)

UNIVERSITY of HOUSTON

NCALM The National Center for Airborne Laser Mapping
University of Houston • University of California, Berkeley

UNIVERSITY of HAWAI'I

PGF

USGS science for a changing world

1. Introduction

Airborne LiDAR (Light Detection And Ranging) systems have become a standard mechanism for acquiring dense high-precision topography, making it possible to perform large scale documentation (100s of km²/day) at spatial scales as fine as a few decimeters horizontally and a few centimeters vertically. However, current airborne and terrestrial LiDAR systems suffer from a number of drawbacks. They are expensive, bulky, require significant power supplies, and are often optimized for use in only one type of mobility platform. It would therefore be advantageous to design a lightweight, compact, and relatively inexpensive multipurpose LiDAR and imagery system that could be used from a variety of mobility platforms – both terrestrial and airborne. The system should be quick and easy to deploy and require a minimum amount of existing infrastructure for operational support. Our research teams have developed a prototype laser scanning system to overcome these issues (Figure 1). We will present system design and development details, along with field experiences and a detailed accuracy analysis of the acquired pointclouds, which show that an accuracy of 3-5 cm (1σ) vertical can be achieved in both backpack and balloon modalities.

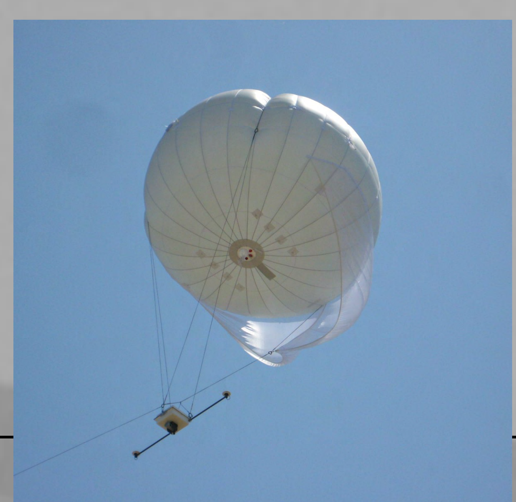

Figure 1: Multipurpose LiDAR System

2. Overview

Figure 2: Tethered Balloon Configuration

We have developed a prototype field deployable compact dynamic laser scanning system ("B-LiDAR") that is configured for use on a variety of mobility platforms, including backpack wearable, unmanned aerial vehicles (e.g. balloons & helicopters), and small off-road vehicles, such as ATVs. The system is small, self-contained, relatively inexpensive, and easy to deploy (Figure 2 and 3).

Figure 3: Backpack Configuration

3. System Description

Instrument Photos © Velodyne & OxTS

The current prototype sensor pod contains a Velodyne HDL-32E LiDAR scanner which contains 32–905 nm lasers, operates at a nominal pulse rate of 700 kHz, and has a range of up to 100 m. It also uses an Oxford Technical Solutions Inertial+2 INS (Inertial Navigation System) with a measurement rate of 100 Hz (Figure 4). Additionally, dual Novatel GNSS (Global Navigation Satellite System) receivers, a ruggedized tablet computer for system control and data logging, and redundant Li-Ion battery packages are part of the system. The current system configuration (including cabling, packaging, and power supply) has a mass of roughly 15 kg and is capable of survey missions of approximately six hours duration (Figure 5).

Accuracy: 2 cm (1σ)
Weight: 2 kg
Dimensions: 15 × 8.5 cm

Accuracy: ω,φ—0.03°; κ—0.1°
Weight: 2.2 kg
Dimensions: 23.4 × 12.0 × 8.0 cm

Figure 4: Velodyne HDL-32E (Left) and OxTS Inertial+2 (Right)

Acquisition & Processing

To produce the highest quality geodetic data, the system has been configured so that all data processing tasks are performed post-mission. Raw data from all sensors (i.e. GNSS, INS, laser scanner) are recorded by the logging and control computer on board the instrument package. After data acquisition, the raw 2-Hz GNSS observations from the onboard receivers are combined with raw measurements from GNSS base station(s) to determine the precise kinematic trajectory for the platform. The GNSS trajectory is then combined with 100-Hz raw inertial measurements in a loosely-coupled Kalman Filter to provide an optimal estimate of vehicle position and attitude. Finally, to generate the final LiDAR point cloud, the estimated platform trajectory and attitude is integrated with the raw range and angle measurements from the laser scanner using software developed by the research team.

Figure 5: Sensor Pod

4. System Calibration

Scanner Calibration

The Velodyne HDL-32E laser scanner is provided with an instrument manufacturer calibration and sample source code that easily allows the user to derive local scanner coordinates for all observations from the laser-detector pairs of the sensor. This enables the user to easily determine the local scanner coordinate pointcloud files. From previous experience, it was found that the relative accuracy of pointclouds could be dramatically improved by performing a rigorous static calibration of Velodyne scanners in order to improve upon the factory scanner calibration [1][2]. A similar approach was used for the scanner in this system, and the resulting calibration showed an approximately 20% improvement in the relative accuracy of the pointcloud obtained by the Velodyne HDL-32E. Given that we are trying to achieve as high an accuracy as possible, a 20% improvement is fairly substantial. Therefore, the improved interior calibration model was used for all of the subsequent data processing and analysis of the system.

Boresight/Lever-Arm Calibration

Additional calibration values are required to accurately transform the point cloud from the scanner's own coordinate system into a global coordinate system. These calibration values are the boresight calibration matrix and the lever-arm offset. Practically, the boresight calibration matrix may only be determined by analysis of geo-referenced point cloud data obtained from the LiDAR scanning system. For our developed system, an approach was used to simultaneously estimate the boresight angles and the horizontal lever-arm components using a non-linear least squares approach [3][4]. The vertical component of the lever-arm is very weakly observable, so it is estimated using the engineering drawings of the subcomponents and overall system assembly. The boresight method used requires a dataset containing numerous planar surfaces that have been collected by the LiDAR system from more than one viewing direction. To collect such a dataset, the instrument package was mounted on the balloon and tethered to a truck, which was then used to pull the balloon past a series of buildings in multiple directions (Figure 6). The planar surface LiDAR data was then manually extracted and used in the least squares adjustment to determine the boresight values. The results showed that the lever arm components were estimated with millimeter-level accuracy, while the angular offsets were estimated within 0.001-0.002° accuracy. These estimated accuracies are well below the noise level of the GNSS/INS navigation trajectory.

Figure 6: Scanning Planar Surfaces

5. Field Testing

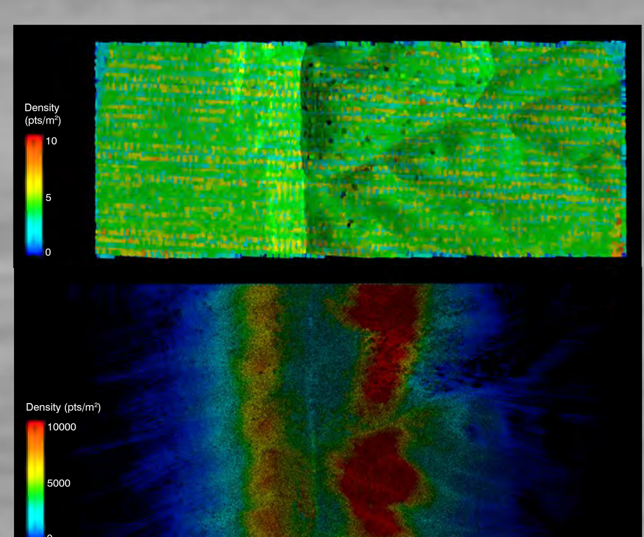

Figure 7: Point Density of B4 Data (Top) and B-LiDAR Data (Bottom)

Sherman Island

We organized a series of tests for the system mounted on a backpack and underneath a tethered 13-ft diameter helium balloon, to assess the accuracy of the system and evaluate the suitability of the system for field operations. Balloon flights were successfully accomplished on May 16-17, 2012, on Sherman Island, near Antioch, CA. For these tests, the balloon was tethered to a light-duty truck and pulled along a levee road at speeds of 7-15 km/hr. For most of the survey, the balloon was at approximately 25 m above ground level (AGL). These survey parameters resulted in a 70-m swath width, and a nominal, point density of 1000-2000 pts/m².

Carrizo Plain

Based on the initial success of Sherman Island, we attempted a more challenging effort designed to demonstrate the range and deployment flexibility of the platform. On May 19-20, 2012, the system was tested, both on the balloon and in backpack mode, on the Carrizo Plain, near Simmler, CA. These tests were a simulation of a rapid-response in the immediate hours after a catastrophic event. Furthermore, the tests were used to evaluate the system's suitability for high resolution mapping in environmentally sensitive or remote regions. After deflating the balloon, we mobilized within a few hours, replenished the Helium supply, and transited over 400 km. We began re-inflating the balloon at dawn and scanned along a well-known section of the San Andreas Fault, near Wallace Creek, on the Carrizo Plain. For the Carrizo balloon tests, a three person crew took advantage of very calm winds to untether the balloon from the pickup truck and walk the B-LiDAR system along the fault at speeds of 3-4 km/hr. For most of the survey, the balloon was at approximately 30 m AGL. These survey parameters resulted in an 80-m swath width, and a nominal point density of 3000 pts/m². For the backpack tests, the instrument package was only 1 m above the ground with a swath width of approximately 4 m, and a point density of approximately 10,000 pts/m². Figure 7 compares B4 airborne LiDAR [5] and B-LiDAR data for a portion of the San Andreas Fault. The figure above shows the respective LiDAR point densities, and Figure 8, below, displays the bare earth DTM from each of the datasets. Note that the point density with B-LiDAR is on average 1000 times higher than the B4 dataset. This high density allows B-LIDAR to produce a more detailed DTM.

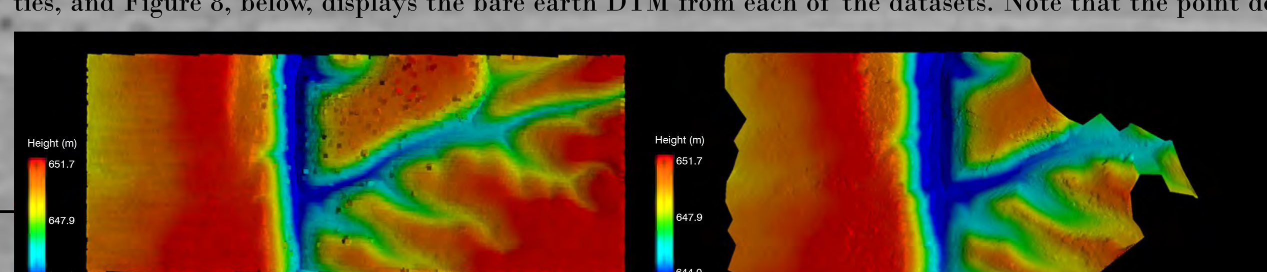

Figure 8: Bare Earth DTM of B4 Data (Left) and B-LiDAR Data (Right)

6. Control Data

Terrestrial laser scanning (TLS) data was acquired at four sites – two on Sherman Island and two along the San Andreas Fault in order to evaluate the accuracy of the pointcloud from the multipurpose system (Figure 9). The scans were acquired with an approximately 1-cm point spacing at 25 m, using a RIEGL VZ-400. The TLS pointclouds were independently geo-referenced to the same geodetic datum as the balloon LiDAR surveys with GNSS positioned retro-reflective targets. Post adjustment of the TLS data to the target points shows 1-2 cm RMS agreement, which gives an overall indication of the quality of the TLS observations.

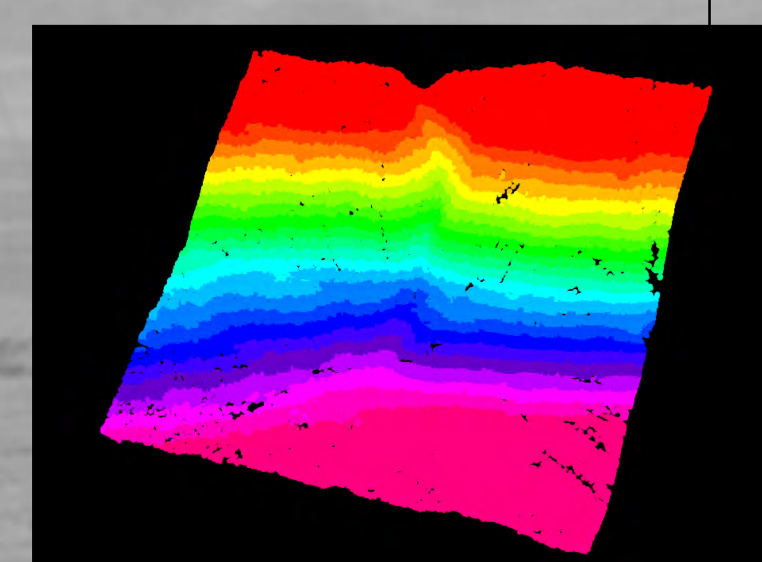

Figure 9: TLS Data Acquired Along Small Offset Channel on Carrizo Plain (10X Elevation Exaggeration)

GNSS Control

For both deployments of the system, two GNSS base stations were set up within the project area to ensure that maximum baseline lengths were always less than 5 km (Figure 10). These local GNSS base stations were also augmented by high rate observations recorded at permanent PBO and USGS GNSS stations near the project area.

Figure 10: GNSS Base Station

7. Results

Table 1: B-LiDAR Pointcloud vs. TLS Observations

(meters)	Minimum	Maximum	Average Magnitude	Mean	RMS	Standard Deviation
Balloon Configuration						
Sherman Island 1	-0.0703	0.1311	0.0327	-0.0032	0.0403	0.0402
Sherman Island 2	-0.1200	0.1315	0.0378	0.0017	0.0472	0.0472
Carrizo Plain 1	-0.1198	0.1336	0.0309	-0.0042	0.0375	0.0373
Carrizo Plain 2	-0.1267	0.1470	0.0369	0.0063	0.0459	0.0455
Backpack Configuration						
Carrizo Plain 1	-0.0815	0.0943	0.0226	-0.0098	0.0284	0.0267
Carrizo Plain 2	-0.0614	0.1012	0.0218	0.0088	0.0299	0.0286

To confirm the accuracy of the prototype's data, in both balloon and backpack configurations, the resulting pointclouds from the system were compared with results from the four TLS scans previously described. For each of the TLS control sites, the kinematic system data was gridded at 1-m intervals over 100 × 100 m sample sites to provide approximately 10,000 observations. Comparisons between the elevations of the gridded kinematic data and the TLS pointclouds were made. Statistics of the comparisons for all sites in both prototype system modes are presented in Table 1. The results clearly show that the TLS data and the airborne kinematic data agree at a level of approximately 4-5 cm (1σ) in the vertical component. The backpack dataset shows slightly better agreement, at approximately 3 cm (1σ). Considering the expected ranging accuracy of the Velodyne scanner (2 cm), and the TLS pointcloud target residuals during geo-referencing (1-2 cm), it would appear that the elevation differences given in Table 1 are at or very near the overall expected noise level. These are very encouraging results and show that the prototype kinematic system is capable of collecting accurately geo-located, and very precise, topographic data.

Future Work

The balloon and tether configuration, along with the backpack design, are currently being optimized. Future goals include extending the scanner's range, upgrading the INS accuracy, and reducing the system's weight (< 8 kg). Also, plans to incorporate an embedded computing module and add a wireless download link are presently being proposed.

References

1. Glennie, C., Lichti, D.D., 2011. Temporal Stability of the Velodyne HDL-64E S2 Scanner for High Accuracy Scanning Applications. Remote Sensing, 3: 539-553.
2. Glennie, C., Lichti, D.D., 2010. Static calibration and analysis of the Velodyne HDL-64E S2 for high accuracy mobile scanning. Remote Sensing, 2: 1610-1624.
3. Glennie, C., 2012. Calibration and Kinematic Analysis of the Velodyne HDL-64E S2 Lidar Sensor. Photogrammetric Engineering & Remote Sensing, 78 (4), 339-347.
4. Skaloud, J., Lichti, D., 2006. Rigorous approach to bore-sight self-calibration in airborne laser scanning. ISPRS Journal of Photogrammetry & Remote Sensing, 61: 47-59.
5. Bevis, M., et al., 2005. The B4 Project: Scanning the San Andreas and San Jacinto Fault Zones. American Geophysical Union, H34B-01.

Acknowledgements

This work was funded by the Public Interest Energy Research (PIER) program of the California Energy Commission, Grant 500-09-035, to the School of Ocean and Earth Sciences and Technology at the University of Hawaii. We thank Juan Mercado, Joel McElroy, and board members of Reclamation District #341, for graciously enabling the field tests on Sherman Island. We thank John Hurl, Kathy Sharum, and Ryan Cooper of the Bureau of Land Management for Carrizo Plain access. We thank Sara Looney, David Phillips, and Chris Walls of UNAVCO for providing the high rate GNSS observations from the PBO GNSS stations and Dan Determan, Aris Aspiotes, and Keith Stark for providing the high rate GNSS observations from the USGS GNSS stations.

Pictures by Ben Brooks & Darren Hauser